Measurement of Elastic Strain Wave Propagation Velocity Using FRSGs along Metallic Rods Subjected to Impact Load

(Aplikasi *FRSG* Untuk Pengukuran Laju Perambatan Gelombang Regangan Elastis Akibat Beban Impak pada Batang Logam)

SUDARISMAN

ABSTRACT

The accuracy of foil resistance strain gauge (FRSG) for strain wave propagation measurement along metallic rods, i.e. aluminium, brass, copper and steel rods, subjected to impact load has been investigated. Hexagonal cross section of 5/8" sides $\times$ 6' long metallic rods have been selected for specimens. At a distance of 8" from one end of each rod, an EA-09-125AD-120 type foil resistance strain gauge with gauge factor of 2.105 and resistance of 120Ω was installed. The rods were then placed on a pair of supports and loaded at the other end surface with an impact loading generated using an impulse hammer. The set up was also instrumented with a typical potentiometer circuit as a signal transducer, and an oscilloscope for signal acquisition. The output signals were then analysed by comparing with their respective theoretical values. The result showed that these FRSGs had demonstrated high accuracy in signal sensing indicated by negligible discrepancies between experimental values on one hand and their respective theoretical values on the other hand.

Keywords : FRSG, accuracy, strain wave propagation, metallic bars.

INTRODUCTION

Bonded strain gauge was firstly introduced by Charles Kearns in 1930s (Starr, 1994). It was a resistor made from combination of carbon, filler and adhesive materials. Next, in 1937 and 1938, Arthur Ruge and Edward Simons independently introduced strain gauges made of fine metal filaments (Starr, 1994). Eventually, FRSGs were introduced in the U.K. and the U.S. in the early 1950. Due to its geometry being foil with a very small cross section, a considerably small length can produce a large magnitude of resistance, and the mechanical characteristic of the specimens under investigation may not be noticeably affected. In addition, its elongation wll exactly be the same as that of the specimen due to its installation being bonded. Therefore, the measurement may be guaranteed for being highly accurate.

Wide variety of strain gauges is currently available in the market. Total thickness of the foil can be found to vary from 2.5 μm (Starr, 1994) to 10 mm with the width and length of the grids to vary from 0.51 mm to 6.35 mm and from 0.38 mm (Anonym, 2010a) to 100 mm (Anonym, 2010b), respectively. In comparison to other types of censors, FRSG possesses some advantages, e.g., high calibration constant stability, high accuracy, small dimension, its set up can be equipped with temperature and lead-wire compensation element, ease of installation and operation, produce linear response in wide range of measurement, can be utilised as sensing device for various transducers, and considerably low price.

Due to its superiority in comparison with other types of sensing device FGRS has widely been accepted as sensing device. Reliability of FRSG for measuring static (Sudarisman, 1998) and dynamic (Sudarisman, 2003) strains of cantilever beams has previously been reported.

The current work deals with the performance and accuracy of FRSG as sensing device for elastic

strain wave propagation along metallic rods. The experimental data being captured from the pulses of elastic wave propagation signals along the rods were then compared to their respective theoretical values. The accuracy of the FRSG was calculated as the degree of discrepancy between experimental and theoretical values. The result can be used as a consideration in selecting sensing device for dynamic strain measurement.

THEORETICAL BACKGROUND

Elastic Strain Wave Propagation

The theoretical velocity of a 1-D elastic strain wave propagation along a slender metallic rod is given as (Meriam, 1980):

$$v_t = (E/r)^{0.5} \text{ (m/s)} \tag{1}$$

where E and r are the elastic modulus (Pa) and density (kg/m^3) of the material under investigation. If time period of the strain wave is given as t (s), then the frequency of the vibration is,

$$f = 1/t \tag{2}$$

If the length of each rod is l(m), then the wave length of the strain wave propagation is,

$$l = 2l \text{ (m)} \tag{3}$$

Thus, the experimental value of strain wave propagation velocity in the rods is given as:

$$v_e = 2l / t \text{ (m/s)} \tag{4}$$

Foil Resistance Strain Gauge Characteristics

Charles Kearns may be the first who introduced strain gauges in 1930s (Starr, 1994). The gauges were in the form of resistors made from combination of carbon, filler and adhesive. Following him, in 1937 and 1938, Arthur C. Ruge and Edward E. Simmons, Jr. independently introduced strain gauges in the form of bonded fine metal. In 1952, Peter J. Scott Jackson invented the foil resistance gages (FRGs) that can be bonded on to the specimen being tested. These FRGs are those that currently most widely used for strain analysis and transducers.

The Measurement Group produces FRSGs whose thickness is only as thin as 2.5 – 5.0 μm, length of 0.2 – 100 mm, and resistance of 60 ? – 5000 ? (Starr, 1994). Any gauges available in the market come with specifications and detail instruction for installation and usage, such that by following them accurate measurement can be obtained. The shorter the applied gauge length the more accurate a measurement, because strain measurement using FRSGs is basically measuring strain state at a point. There are advantageous of FRSGs, e.g. stability of the constant of their circuitry, high accuracy, small in dimension, the change in temperature and the length of their lead wire can be compensated by employing compensating circuit, ease of installation and operation, linear response over a wide range of strain measurement, use ability in various types of transducer, and cost effectiveness.

Calibration is generally required for any change in circuitry variable. For signal amplifying purpose, the circuit may be equipped with a potentiometer circuit or Wheatstone bridge circuit. If a potentiometer circuit is utilised, the circuit will be equipped with a switch for connecting and disconnecting the calibration resistor.

Gauge installation is relatively easy and not time consuming. After being cleaned from mechanical and chemical contaminants, the surface where the gauge will be installed is applied with adhesive, the gauge is carefully placed, and a light press is applied, in order to obtain a thin layer of adhesive, on to the gauge for a few minutes until the adhesive completely cured.

Potentiometer Circuit Calibration

Due to its faster response in comparison with those of Wheatstone bridge circuit, a potentiometer circuit, as presented in Figure 1, has been selected as the transducer in this experiment. This transducer converts elastic strain wave propagation signal into electrical voltage. In order to produce accurate measurement, the circuit has to be calibrated prior to being used for measuring elastic wave propagation signal.

The magnitude of resistance and current between points A and B are, respectively:

$$i = E_i / (R_b + R_{AB}) = E_i / (R_{AB} + R_b) \tag{5}$$

When the switch S is off, i.e., loading-free state, then,

$$R_{AB} = R_g \tag{6a}$$
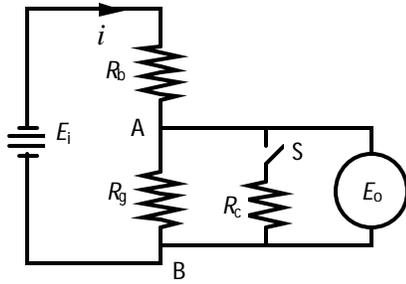
FIGURE 1. Schematic diagram of a potentiometer circuit

Note for Figure 1:

E_{AB} = E_o for loading-free state
E_{AB} = E_c for calibration loading state
E_{AB} = E_g for actual loading state.
E_i = input voltage (V)
i = the magnitude of current in the circuit (A)
R_{AB} = resistance between points A and B (?)
R_b = ballast resistance (?)
R_g = strain gauge resistance (?)
R_c = calibrating resistance (?)
E_{AB} = output voltage (V)
DR_g = the change of resistance of the strain gauge due to loading (?)

and

$$E_{AB} = E_o = i\, R_{AB} = E_i / (1 + R_b/R_g) \tag{6b}$$

When the switch S is on, *i.e.* calibration state, then:

$$R_{AB} = (R_g \cdot R_c) / (R_g + R_c) \tag{7a}$$

$$i = E_i / (R_b + R_{AB})$$

$$= E_i \cdot (R_g \cdot R_c) / [R_b \cdot (R_g \cdot R_c) + R_{AB}] \tag{7b}$$

Thus,

$$E_{AB} = E_c = i\, R_{AB}$$

or

$$E_c = E_i R_c / [(1 + R_b/R_g) R_c + R_b] \tag{8}$$

In measuring state where the switch S is off, then:

$$R_{AB} = R_g + DR_g \tag{9a}$$

$$i = E_i / (R_B + R_{AB}) = E_i / (R_b + R_g + DR_g) \tag{9b}$$

Thus,

$$E_g = E_{AB} = i\, R_{AB},$$

or

$$E_g = E_i (1 + DR_g/R_g) / (1 + R_b/R_g + DR_g/R_g) \tag{10}$$

If the changes of output voltage during the calibration and during loading are DE_c and DE_g, respectively, then:

$$DE_c = E_o - E_c \tag{11a}$$

$$E_g = E_o - DE_g \tag{11b}$$

If the amplitudes of the calibration and measurement signals are h_c (mm) and h (mm), respectively, then the values of calibration factor, F_c (mV/mm), and the output voltage, E_g (mV) would be given as:

$$F_c = (E_o - E_c) / h_c \tag{12a}$$

$$E_g = E_o - (h/h_c)(E_o - E_c) \tag{12b}$$

On the substitution of equation (12b) into equation (10) produces the value of (DR_g/R_g). Recalling the definition of gauge factor, F_g, (Dally et al., 1993) as:

$$F_g = (DR_g/R_g) / e \tag{13a}$$

The magnitude of strain being measured, e, can be calculated as follows:

$$e = (DR_g/R_g) / F_g \tag{13b}$$

EXPERIMENT

Specimens and Instrumentation

The specimens used in the current experiment are four metallic rods made from different materials, *i.e.* aluminium, brass, copper and steel. The rods are of 72 (in.) long, and possessing hexagonal cross section of $1^1/_4$ (in.) length of major diagonal. An EA-09-125AD-120 type of foil resistance strain gauge (FRSG), supplied by the Micro-measurement Ins., was installed in each of the rods at a point of 6 (in.) from one of their respective ends. The resistance of the gauge is 120 (?), and the gauge factor is 2.105. The main physical and mechanical properties of the specimen materials have been presented in Table 1.

TABLE 1. Mechanical properties of the specimens

Material	Density, r (g/cm^3)	Young's modulus, E (GPa)	Poisson's ratio, n
Aluminium 7075-T6	2.80	70	0.33
Brass, Red 80Cu-20Zn	8.60	100	0.34
Copper, hard	8.90	120	0.33
Steel	7.85	210	0.28

SOURCE: Gere & Timoshenko (1991)

Experimental Set-up

The schematic illustration of the set-up for data acquisition has been depicted in Figure 2.
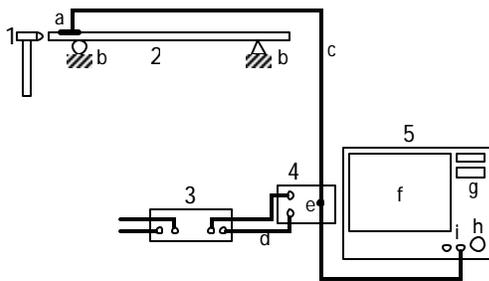
FIGURE 2. Experimental set-up

1. Impuls hammer
2. Specimen, equipped with: (a) FRSG, (b) support system, and (c) co-axial lead-wire
3. Power supply
4. Potentiometer circuit, equipped with: (d) input voltage terminals, and (e) calibration switch
5. Oscilloscope, with: (f) output signal display, (g) output signal adjustment, (h) time display adjustment, and (i) dual-channel input terminal

Experimental Procedure

The output voltage of the power supply was set to 6 (V), and the vertical grid lines representing time in the oscilloscope display was set to 500 (ms). Next, one of the specimens and the impulse hammer were connected to the potentiometer circuit. After the 'TRIGGER' button of the oscilloscope being pressed, the display would send an 'awaiting signal' message indicating that the oscilloscope was ready to take any input signals. The cross section of one of the specimen ends was then hit using the impulse hammer. In order to avoid bending effect, the hammer trajectory must be perpendicular to the surface when hitting it. The strain wave propagation pattern would be displayed in output signal monitor of the oscilloscope. Immediately press the 'STOP' button to save the image being displayed. The image would then be traces on a peace of transparent plastic film.

The same procedure, as above, was then applied to each of the other specimens. The calibration signal as depicted in Figure 3 can be obtained by pressing the 'CALIBRATING SIGNAL' button while the oscilloscope was displaying any one of the strain wave propagation signals. The elastic strain wave propagation signals of the four specimens have been presented in Figure 4.

RESULT AND DISCUSSION

Calibration for Strain Measurement

Figure 3 below presents an elastic strain wave propagation calibration signal obtain from the experiment.
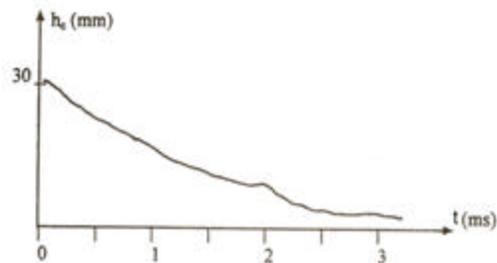
FIGURE 3. Elastic strain wave propagation calibration signal

It shows that the maximum amplitude, h_c, is 31 (mm). Referring to Figure 1, the values of the variables applied in this current experiment are,

$E_i = 6$ (V) $R_g = 120$ (Ω)

$R_b = 120$ (Ω) $R_c = 120\,000$ (Ω)

On the substitution of these values into equations (6a), (8) and (10), yields,

$E_o = 3$ (V)

$E_c = 2.998\,501$ (V)

$$E_g = 6\,(1 + \Delta R_g/R_g) / (2 + \Delta R_g/R_g) \qquad (14)$$

Next, substitution of the values of E_o, E_c and h_c into equation (12a) gives the calibration factor, F_c is equal to 0.046 850 (mV/mm).

Elastic Strain Wave Propagation Speed

Figure 4 below shows strain wave propagation signals.

(a)

(b)

(c)

(d)
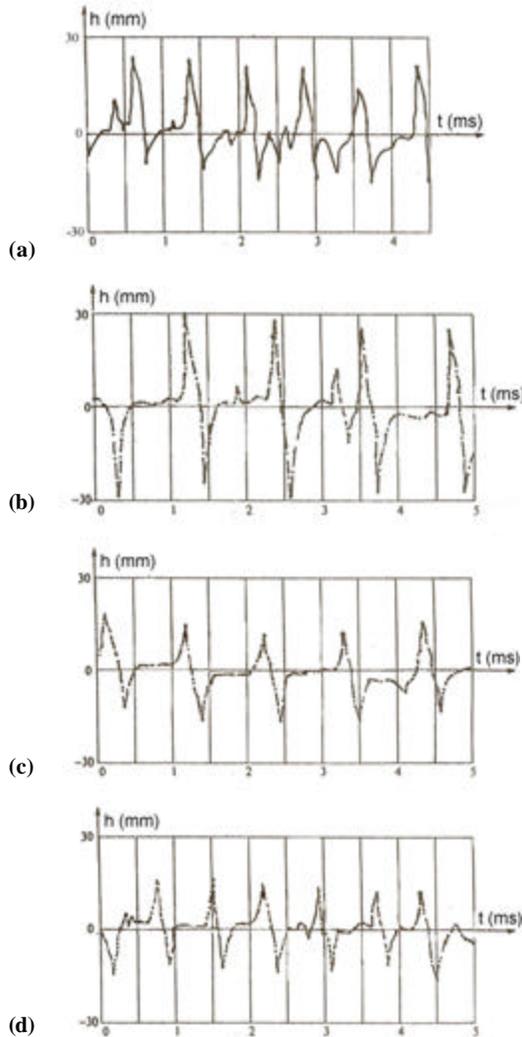
FIGURE 4. Elastic strain wave propagation signals.
(a) Aluminium bar, (b) Brass bar, (c) Copper bar, and (d) Steel bar

A vertical grid space shown in Figure 4 represents 5 (ms) time interval. It shows that the signals produced by the brass and copper bars, Figures 4(b) and 4(c), possess an almost equal time period, so do those of the aluminium and steel bars, Figures 4(a) and 4(d). Observing the signal amplitudes, h_{max}, the largest one was exhibited by the elastic strain wave propagation of the brass bar, followed by that of the aluminium, and either that of the copper or steel bar.

By measuring each horizontal distance between two adjacent peak signals and multiplying them with its time scale, *i.e.* 5 (ms/grid), we can obtain the time period required by each individual strain wave to propagate along each metallic rod, *i.e.* to travel a one complete cycle, as has been presented in column (2) of Table 2. The values of v_t, as presented in column (3) were calculated by employing equations (1) to (4), applying the constants given in Table 1, and the value for g = 9.87 (m/s^2). Next, the values of v_e presented in column (4) were obtained by multiplying the values presented in column (2) with the length of each of the metallic bars, *i.e.* 72 (ft).

TABLE 2. Elastic strain wave propagation speed

Material	Time period, t (ms)	Theoretical speed, v_t (m/s)	Experimental speed, v_e (m/s)	$(v_e - v_t)/v_t$ 100%
(1)	(2)	(3)	(4)	(5)
Aluminium 7075-T6	0.740	4990.9	4941.7	-0.986
Brass, Red 80Cu-20Zn	1.132	3336.9	3231.4	-3.161
Copper, hard	1.043	3637.7	3505.8	-3.626
Steel	0.732	5061.2	4994,.8	-1.312

The discrepancies presented in column (5) were considerably small, less then 4%. Experimental environment, in which the experiment were carried out might not appropriately be shielded, such as vibration of other devices, electrical and electromagnetic fields may be responsible fot this discrepancy. Such error can also come from data acquisition system, such as the length of lead-wire being used, the quality of terminal connections, as well as from the homogeneity of the materials that may affect their physical and mechanical properties.

Although the discrepancies are considerably small that indicates that strain gages demonstrated an acceptable reliability and accuracy for measuring propagation phenomena, further investigation concerning the sources of error may be worth doing. In order to enable to determine the source of such error, a study on the chemical composition and micro-structure of the material being used need to be carried out. In addition, experimental environment shielding and the sensitivity and

accuracy of the data acquisition system should also be a major concern.

TABLE 3. Maximum elastic strain calculation

Material	h_{max} (mm)	E_g (V)	DR_g/R_g ($\times 10^{-3}\Omega/\Omega$)	e_{max} ($\mu\varepsilon$)
(1)	(2)	(3)	(4)	(5)
Aluminium 7075-T6	24.0	2.9988	-2.0020048	-951.071145
Brass, Red 80Cu-20Zn	31.0	2.9985	-2.0020050	-951.071250
Copper, hard	18.5	2.9991	-2.0020046	-951.071063
Steel	16.0	2.9992	-2.0020045	-951.071026

Maximum amplitudes of the signals representing the maximum strain occurred in each bars can be obtained by measuring the h_{max} of each signal as have been presented in column (2) of Table 3. Recall that $E_o = 3$ (V) and $E_c = 2.998\,501$ (V), and substituting the values of h_{max} as presented in column (2) into equation (12b) will produced the output voltage when performing the measurement, E_g, as presented in column (3). Next, the substitution of E_g into equation (14) yields the values of DR_g/R_g as presented in column (4). Finally, the values of maximum strain, e_{max}, as presented in column (5) were obtained by employing equation (13b) for the appropriate values presented in the previous columns.

Column (5) of Table 3 reveals that an approximately the same magnitude of triggering impulses produced insignificantly different magnitude of elastic strain among the sample bars made of different metals. These differences can only be observed after the third decimal digits of strain presented in micro-strain unit. It suggested that the differences are only in the order of 10^{-10} or 10^{-8} per cent, which is insignificant. Further conclusion that can be drawn is that the strain gages exhibited high accuracy for measuring elastic strain wave propagation along metallic bars.

CONCLUSION

It can be concluded that the strain gauges utilized as sensing devices for elastic strain wave measurement have demonstrated high accuracy, consistency and reliability. The maximum discrepancies from their respective theoretical values are only 3.626% for propagation velocity measurement, and 10^{8}% for the magnitude measurement of elastic strain wave.

REFERENCES

Anonym. (2010a). *Technical data for general-use strain gages*. Raleigh: Micro-Measurement Inc.

Anonym. (2010b). *Special use sensors – concrete embedment strain gages*. Raleigh: Micro-Measurement Inc.

Dally, J.W., Riley, W.F. & McConnel, K.G. (1993). *Instrumentation for engineering measurements*. New York: John Wiley and Sons.

Gere, J.M. & Timoshenko, S.P. (1991). *Mechanics of materials* (3rd ed.). London: Chapmann & Hall.

Meriam, J.L. (1980). *Dynamics*. New York: John Wiley & Sons.

Starr, J.E. (1994). Basic strain gage characteristics. In Hannah, R.L. and Reed, S.E. (Ed.), *Strain Gage User's Hanbook* (pp. 1-78). London: Chapmann & Hall,.

Sudarisman. (1998). Kecermatan strain gage sebagai alat pungut sinyal regangan statis balok kantilever. *Arena Almamater*, *12*(45), 1-12.

Sudarisman. (2003). Pola regangan dinamis pada balok kantilever akibat getaran berfrekuensi rendah. *Semesta Teknika*, *6*(1), 60-72.

AUTHOR:

Sudarisman

Department of Mechanical Engineering, Faculty of Engineering, Universitas Muhammadiyah Yogyakarta, Jalan Lingkar Selatan, Bantul 55183, Yogyakarta, Indonesia.

Email: sudarisman05@yahoo.com.au